Power System Analysis Using Space–Vector Transformation

José M. Aller, Alexander Bueno, and Tomás Pagá

***Abstract*—In this paper, the space–vector transformation used in machine vector control is applied to power system analysis. The proposed method is used to model electric machines, power electronic converters, transformers, and transmission lines and to analyze power sources and loads with different connections (delta and wye). This method can also be applied to analyze steady-state (or transient phenomena) and unbalanced sources, including harmonics. Models obtained with this method are as simple as those of the per-phase approach. With the space–vector transformation, instantaneous active and reactive power concepts can be generalized, and new power system control strategies can be developed when power electronic converters are used. Steady-state, transient behavior, and harmonic analyses examples and applications are presented to illustrate the performance and advantages of the proposed method. This method can be extended to unbalanced systems (e.g., unsymmetric faults) using instantaneous symmetrical components in polyphase balanced circuits.**

***Index Terms*—AC machines, circuit simulation, induction machines, power electronics, power system harmonics, power system simulation, rectifiers, time domain analysis, transformers, transmission line matrix methods.**

I. Introduction

POWER SYSTEMS have been traditionally analyzed using matrix transformations (Clark, Fortescue, Park, etc.) [1]–[6]. The modal representation method decouples symmetric power system equations. This technique has been widely used to model electric systems in steady-state (underbalanced and unbalanced operations) and to analyze transients (dynamics and harmonics). However, modal decoupling of the system equations can be hard in complex polyphase networks. Hence, some authors have used nontransformed coordinates for power system analysis [7].

During the last decade, the control of induction machines using space–vector methods and field orientation has been thoroughly developed [8]–[13]. Space–vector transformations are derived from symmetrical components transformation [3], [5], [13], and they lead to a concise representation because the zero-sequence model is not needed when the neutral is not connected; the negative-sequence model is a complex conjugate representation of the space–vector model [10], [11]. One advantage of the space–vector transformation for induction machine analysis is the reduction from six real equations (three for the stator and three for the rotor) to a pair of complex equations (one for the stator and one for the rotor). The other advantage is the representation of three time-varying quantities with one space-time complex variable.

Symmetrical components transformation decouples symmetric and cyclic polyphase systems. Symmetric systems such as ideally transposed transmission lines, transformers, and loads can be decoupled by any modal transformation [4], [5], but the main advantage of symmetrical components transformation is the decoupling of cyclic systems such as induction motors and cylindrical rotor synchronous machines. Salient-pole synchronous machines, unbalanced loads, long nontransposed lines, and unsymmetrical faults cannot be uncoupled by any generic transformation. Park's transformation [2], [14] or any other rotational transformation can be used to simplify the salient-pole synchronous machine model, but in these models there is a strong coupling between the transformed coordinates (dq). Since, space–vector transformation is directly derived from symmetrical components, it can also be applied to decouple the power system equations for balanced systems.

In [15]–[18], a new rectifier control technique has been developed to reduce harmonic distortion, increase power factor, and improve power quality. The control scheme is based on space–vector theory (active rectification) and requires insulated gate bipolar transistor or gate turn off thyristors power switches. Space–vector control is simpler than other control techniques, and it simplifies the analysis of ac/dc converters. Interconnection between the power system and the active rectifier can also be modeled using the space–vector transformation. For this purpose, power system representation using space vectors is a very useful approach.

II. Definitions

Traditionally, power systems have been analyzed using symmetrical components, Clark transformation, or any other modal transformation [1], [3]–[6]. These polyphase transformations decouple symmetric and cyclic polyphase systems. In balanced power systems or in systems without a neutral return, the zero-sequence component is zero. Positive and negative sequences have similar behavior, especially in symmetric polyphase systems. During the last decade, the space–vector transformation has been widely applied in the dynamic control of electrical machines [8]–[12]. The space–vector transformation is defined as

$$\vec{\mathbf{x}} \equiv \sqrt{\frac{2}{3}}\left[1 \quad e^{j2\pi/3} \quad e^{j4\pi/3}\right] \cdot \begin{bmatrix} x_a(t) \\ x_b(t) \\ x_c(t) \end{bmatrix} = x_\alpha(t) + j\, x_\beta(t) = x(t)\, e^{j\xi(t)}. \tag{1}$$

Manuscript received August 1, 2000; revised February 26, 2002. This work was supported in part by the CONICIT under Grant S1-97001762.

The authors are with Universidad Simón Bolívar, Caracas, 1080 Venezuela, (e-mail: jaller@usb.ve; bueno@usb.ve; tpaga@usb.ve).

Digital Object Identifier 10.1109/TPWRS.2002.804995

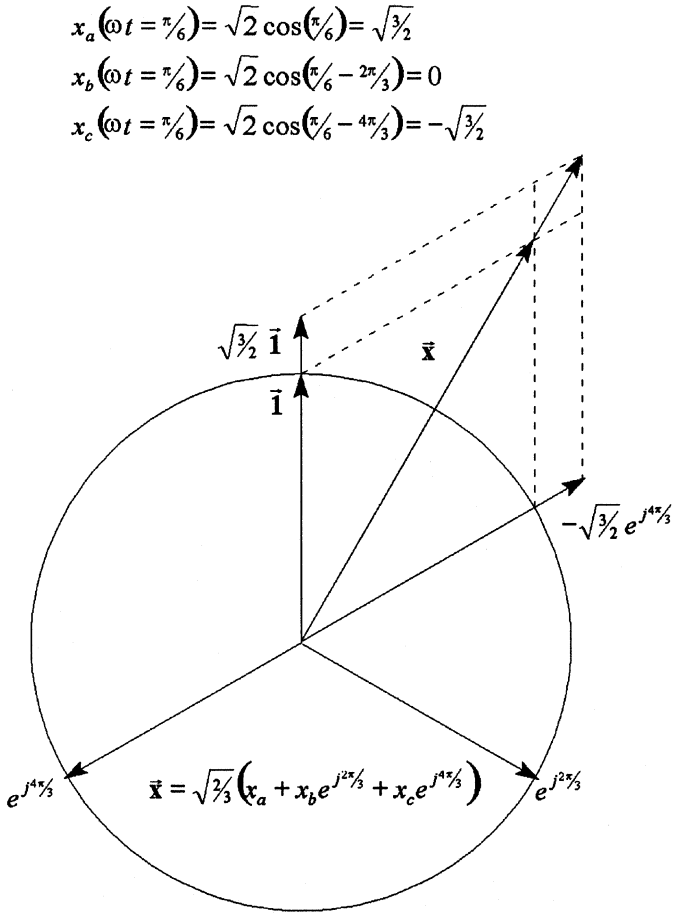

Fig. 1. Graphical interpretation of space–vector transformation.

The coefficient $\sqrt{2/3}$ is needed to conserve power between the coordinate systems. The factor $1/\sqrt{3}$ is obtained from the Hermitian symmetrical components transformation [5], [14], and $\sqrt{2}$ is necessary to produce the same instantaneous active power in the original coordinates and the space–vector frame in a balanced system. The space–vector transformation is illustrated in Fig. 1.

Since the instantaneous power must match the conventional complex power definition under balanced steady-state conditions, it is necessary to express it as [19]–[21]

$$\vec{s}(t) \equiv \vec{v}(t) \cdot \vec{i}^{*}(t) = p(t) + jq(t) \tag{2}$$

where $\vec{v}\,(t)$ and $\vec{i}^{*}\,(t)$ are space vectors defined as

$$\vec{v}\,(t) \equiv \sqrt{\frac{2}{3}}\,[1 \quad e^{j2\pi/3} \quad e^{j4\pi/3}] \cdot \begin{bmatrix} v_a\,(t) \\ v_b\,(t) \\ v_c\,(t) \end{bmatrix} \tag{3}$$

$$\vec{i}^{*}\,(t) \equiv \sqrt{\frac{2}{3}}\,[1 \quad e^{j4\pi/3} \quad e^{j2\pi/3}] \cdot \begin{bmatrix} i_a\,(t) \\ i_b\,(t) \\ i_c\,(t) \end{bmatrix}. \tag{4}$$

Substituting for the voltage and current space vectors in (2), instantaneous power can be expressed in abc variables as

$$\begin{aligned} \vec{s}(t) &= p\,(t) + j\,q\,(t) \\ &= [v_a \cdot i_a + v_b \cdot i_b + v_c \cdot i_c] \\ &\quad + j\frac{\sqrt{3}}{3}\,[i_a \cdot v_{bc} + i_b \cdot v_{ca} + i_c \cdot v_{ab}]\,. \end{aligned} \tag{5}$$

The above expression (5) is valid under all operating conditions, three- or four-wire systems, transient and steady-state operation, balanced and unbalanced conditions, and sinusoidal or nonsinusoidal waveforms. The real part in (5) is identical to the classical instantaneous power definition; but the imaginary part is not so well known, and it disagrees in some special cases with the classical definition. In a balanced steady-state sinusoidal three-phase system, the instantaneous active and reactive powers are time invariant, because the voltage and current space vectors (3) and (4) have constant amplitude, and their relative phase is also constant. In this condition, the classical and the vector definitions agree, but under nonsinusoidalconditions (or in unbalanced systems), the classical and vector power definitions are different.

A physical interpretation of (2) can be given by considering the relationships that exist between electromotive force e and electric field intensity $\vec{\mathbf{E}}$ on one hand and, on the other hand, magnetic field intensity $\vec{\mathbf{H}}$ and current i. The Poynting vector $\vec{\mathbf{S}}$ is the cross-product of the electric field intensity $\vec{\mathbf{E}}$ and the magnetic field intensity $\vec{\mathbf{H}}$, i.e., $\vec{\mathbf{S}} = \vec{\mathbf{E}} \times \vec{\mathbf{H}}$. This space-time vector represents the power flow per unit area of the electromagnetic field. For example, at a given point in the air-gap of a rotating electric machine, the Poynting vector $\vec{\mathbf{S}}$ has two components: one in the radial direction that determines the active power flow and the other in the tangential direction that maintains the rotating electromagnetic field required during the operation. In a three-phase transmission line, the phenomena is similar; but the instantaneous active power $p(t)$ corresponds to the longitudinal component of the Poynting vector, and the reactive power $q(t)$ is related to the tangential or rotational component of this vector. As the current i and the magnetic field intensity $\vec{\mathbf{H}}$ are related through Ampere's Law, and the electromotive force e is obtained by integration of the electric field intensity $\vec{\mathbf{E}}$, it is reasonable to think that the instantaneous active power $p(t)$ is related to the radial component of the Poynting vector $\vec{\mathbf{S}}$ and the instantaneous reactive power $q(t)$ to the tangential component of this vector.

III. Power System Models

A. Delta–Wye Sources and Loads

Fig. 2 shows a load or simple source in delta or wye connection; in a balanced system, the neutral current is zero. Passive loads are modeled assuming zero voltage in the power source. Active loads and simple generators can be modeled using balanced voltages in the polyphase source.

Delta connection [Fig. 2(a)] can be modeled as follows:

$$\begin{bmatrix} v_{ab} \\ v_{bc} \\ v_{ca} \end{bmatrix} = \begin{bmatrix} v_1 \\ v_2 \\ v_3 \end{bmatrix} + \begin{bmatrix} Z(p) & M(p) & M(p) \\ M(p) & Z(p) & M(p) \\ M(p) & M(p) & Z(p) \end{bmatrix} \begin{bmatrix} i_{ab} \\ i_{bc} \\ i_{ca} \end{bmatrix} \tag{6}$$

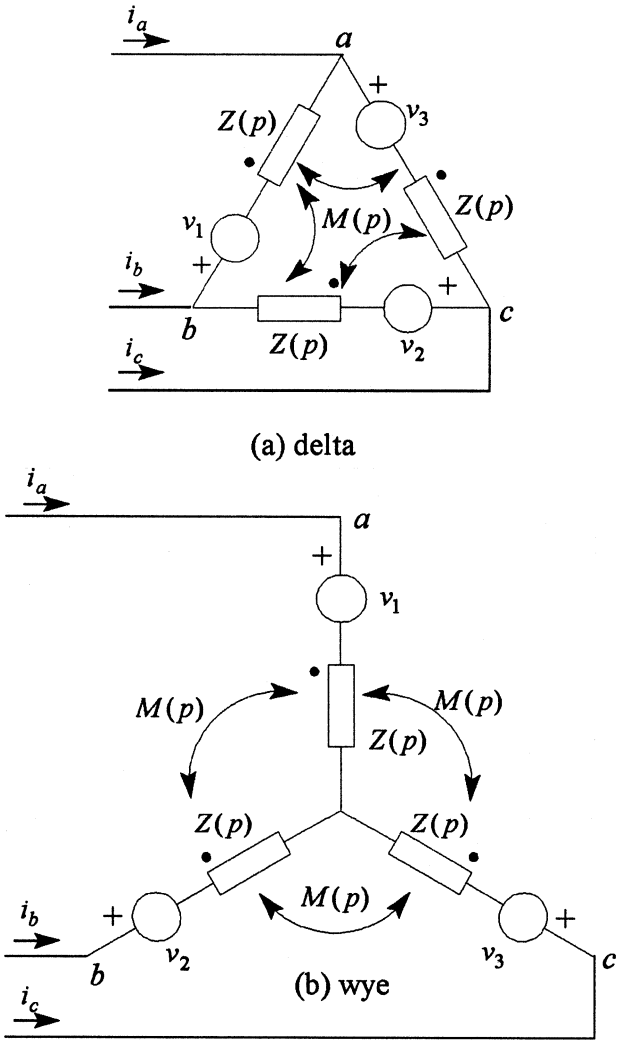

Fig. 2. Operational loads and simple sources connected in (a) Delta, and (b) Wye.

$$\begin{bmatrix} i_a \\ i_b \\ i_c \end{bmatrix} = \begin{bmatrix} 1 & 0 & -1 \\ -1 & 1 & 0 \\ 0 & -1 & 1 \end{bmatrix} \begin{bmatrix} i_{ab} \\ i_{bc} \\ i_{ca} \end{bmatrix}. \tag{7}$$

Applying the space–vector transformation to (6) and (7) results in the following expression:

$$\vec{v}_s = \frac{e^{-j\pi/6}}{\sqrt{3}}\vec{e}_s + \frac{Z(p) - M(p)}{3}\vec{i}_s \tag{8}$$

where

$$\vec{e}_s \equiv \sqrt{\frac{2}{3}}\left[1 \quad e^{j2\pi/3} \quad e^{j4\pi/3}\right] \cdot \left[v_1 \quad v_2 \quad v_3\right]^t.$$

Equation (8) is the space–vector model for delta connection. The space vector of the electromotive force is a line to neutral voltage with a 30° lag. The factor "3" that divides the impedance in (8) is similar to delta–wye transformation.

Wye connection [Fig. 2(b)] can be modeled as follows:

$$\begin{bmatrix} v_a \\ v_b \\ v_c \end{bmatrix} = \begin{bmatrix} v_1 \\ v_2 \\ v_3 \end{bmatrix} + \begin{bmatrix} Z(p) & M(p) & M(p) \\ M(p) & Z(p) & M(p) \\ M(p) & M(p) & Z(p) \end{bmatrix} \begin{bmatrix} i_a \\ i_b \\ i_c \end{bmatrix}. \tag{9}$$

Applying space–vector transformation to (9), the following equation can be obtained:

$$\vec{v}_s = \vec{e}_s + (Z(p) - M(p))\,\vec{i}_s. \tag{10}$$

Equation (10) represents the space–vector model for wye connection.

B. Transmission Line Model

In Fig. 3, a three-phase medium-length transmission line model is shown, including line–line and line–ground capacitances, self- and mutual inductances and resistance. Using (8) and (10), the transmission line model in space–vector coordinates can be obtained using generalized circuit parameters (A, B, C, D) as

$$\begin{bmatrix} \vec{v}_{\text{in}} \\ \vec{i}_{\text{in}} \end{bmatrix} = \begin{bmatrix} A(p) & B(p) \\ C(p) & D(p) \end{bmatrix} \begin{bmatrix} \vec{v}_{\text{out}} \\ \vec{i}_{\text{out}} \end{bmatrix} \tag{11}$$

where

$$\begin{aligned} A(p) &= 1 + R_L(3C_M + C_G)p + (L_L - M_L)(3C_M + C_G)p^2 \\ B(p) &= R_L + (L_L - M_L)\,p \\ C(p) &= (3C_M + C_G + R_L(3C_M + C_G)^2 p + \\ &\quad + (L_L - M_L)(3C_M + C_G)^2 p^2)p \\ D(p) &= A(p). \end{aligned}$$

Equation (11) represents the space–vector model of the transmission line. The same procedure can be applied to long transmission lines introducing the space–vector definition into the differential equations that model the multiport system. The model obtained using symmetrical components is identical to the model obtained using space–vector transformation.

C. Transformer Model

An ideal wye-delta transformer is shown in Fig. 4. Wye-delta connections can be analyzed using space vectors as shown in the following:

$$e_{x_1} = a \cdot e_{x_2} \quad e_{y_1} = a \cdot e_{y_2} \quad e_{z_1} = a \cdot e_{z_2} \tag{12}$$

where

$$\begin{aligned} a &= \frac{N_1}{N_2} \\ \begin{bmatrix} v_{ab_1} \\ v_{bc_1} \\ v_{ca_1} \end{bmatrix} &= \begin{bmatrix} 1 & -1 & 0 \\ 0 & 1 & -1 \\ -1 & 0 & 1 \end{bmatrix} \begin{bmatrix} e_{x_1} \\ e_{y_1} \\ e_{z_1} \end{bmatrix} \\ &= \begin{bmatrix} a & -a & 0 \\ 0 & a & -a \\ -a & 0 & a \end{bmatrix} \begin{bmatrix} e_{x_2} \\ e_{y_2} \\ e_{z_2} \end{bmatrix} \end{aligned} \tag{13}$$

$$\begin{bmatrix} v_{ab_2} \\ v_{bc_2} \\ v_{ca_2} \end{bmatrix} = \begin{bmatrix} 1 & 0 & 0 \\ 0 & 1 & 0 \\ 0 & 0 & 1 \end{bmatrix} \begin{bmatrix} e_{x_2} \\ e_{y_2} \\ e_{z_2} \end{bmatrix}. \tag{14}$$

Applying the space–vector transformation to (13) and (14), the following expressions can be obtained:

$$\vec{v}_1 = \sqrt{3} \quad a \quad e^{j\pi/6} \cdot \vec{v}_2. \tag{15}$$

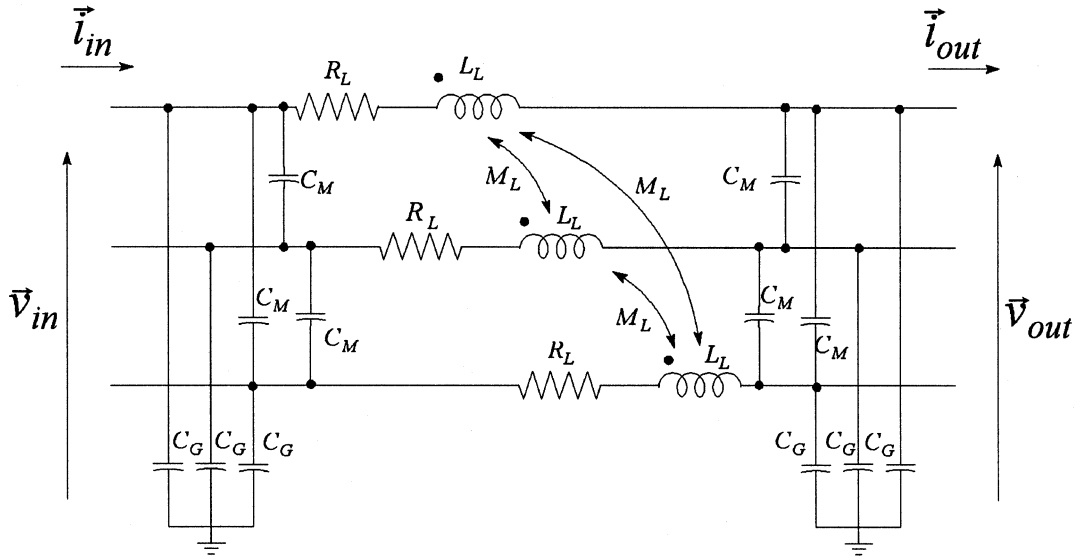

Fig. 3. Medium-length transmission line model.

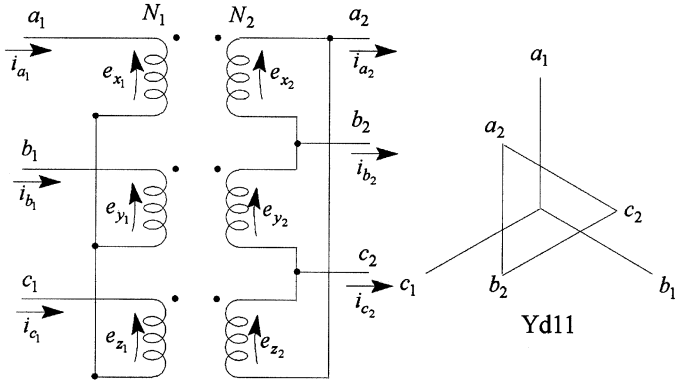

Fig. 4. Ideal three-phase wye-delta transformer.

A nonideal transformer can be modeled using coupled circuit theory applied to the load and source models developed in (6)–(10). Other power transformers such as zig-zag, autotransformers, phase shifting transformers, or multiwinding transformers can be easily analyzed using space–vector transformation. Equation (15) shows the simplicity of the model, for the analysis of steady state, transients, or harmonics. In steady state, the results agree with the classical voltage equations obtained using sequence components.

D. Induction Machine Model

A model for a three-phase induction machine is shown in Fig. 5. Neglecting the effects of magnetic saturation, eddy currents, nonsinusoidal magnetomotive force distribution, and slotting, the induction machine model equations in the original windings frame can be written as [13]

$$\begin{bmatrix}\mathbf{v}_s\\ \mathbf{v}_r\end{bmatrix}=\begin{bmatrix}\mathbf{R}_s & \mathbf{0}\\ \mathbf{0} & \mathbf{R}_r\end{bmatrix}\begin{bmatrix}\mathbf{i}_s\\ \mathbf{i}_r\end{bmatrix}+p\left[\begin{bmatrix}\mathbf{L}_{ss} & \mathbf{L}_{sr}\\ \mathbf{L}_{rs} & \mathbf{L}_{rr}\end{bmatrix}\begin{bmatrix}\mathbf{i}_s\\ \mathbf{i}_r\end{bmatrix}\right] \quad (16)$$

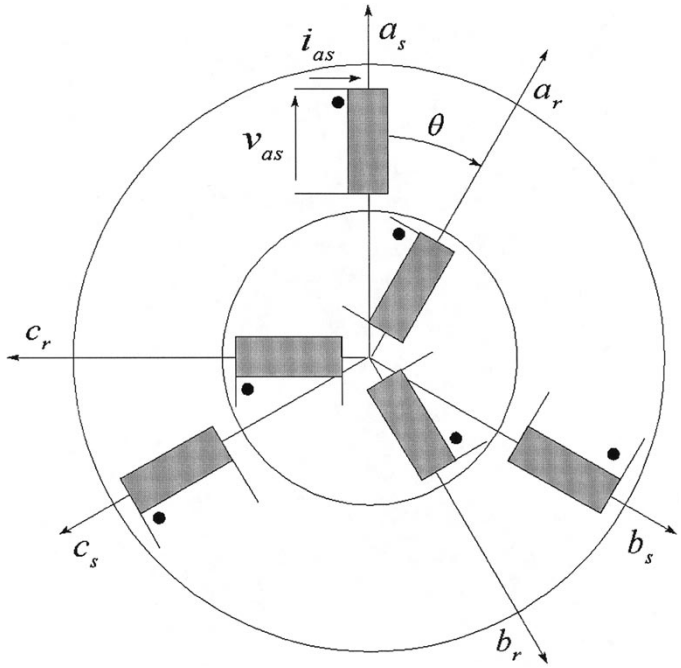

Fig. 5. Three-phase induction machine.

and

$$T_e - T_m = J\cdot\ddot{\theta}+\alpha\cdot\dot{\theta} \quad (17)$$

where

$$\lambda=\mathbf{L}(\theta)\cdot\mathbf{i}=\begin{bmatrix}\mathbf{L}_{ss} & \mathbf{L}_{sr}\\ \mathbf{L}_{rs} & \mathbf{L}_{rr}\end{bmatrix}\cdot\begin{bmatrix}\mathbf{i}_s\\ \mathbf{i}_r\end{bmatrix}$$

$$\mathbf{R}=\begin{bmatrix}\mathbf{R_s} & \mathbf{0}\\ \mathbf{0} & \mathbf{R_r}\end{bmatrix}=\begin{bmatrix}R_s\cdot\mathbf{U} & \mathbf{0}\\ \mathbf{0} & R_r\cdot\mathbf{U}\end{bmatrix}$$

$$\mathbf{L}_{ss}=\mathbf{L}_s+\mathbf{L}_{\sigma s}=L_s\mathbf{S}+L_{\sigma s}\mathbf{U}$$

$$\mathbf{L}_{rr}=\mathbf{L}_r+\mathbf{L}_{\sigma sr}=L_r\mathbf{S}+L_{\sigma r}\mathbf{U}$$

$$\mathbf{L}_{sr}=\mathbf{L}_{rs}^t=L_{sr}\mathbf{C}$$

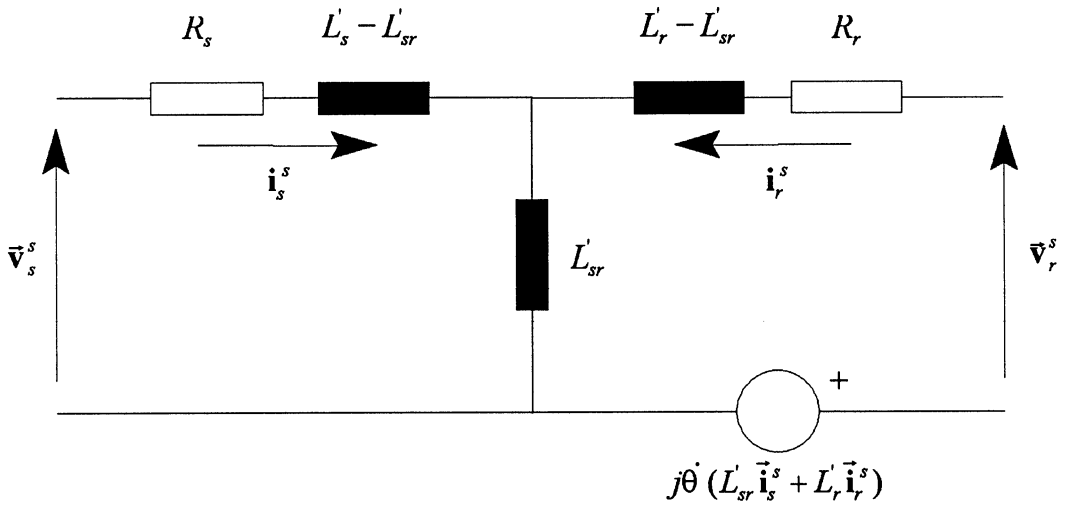

Fig. 6. Space–vector model of the induction machine.

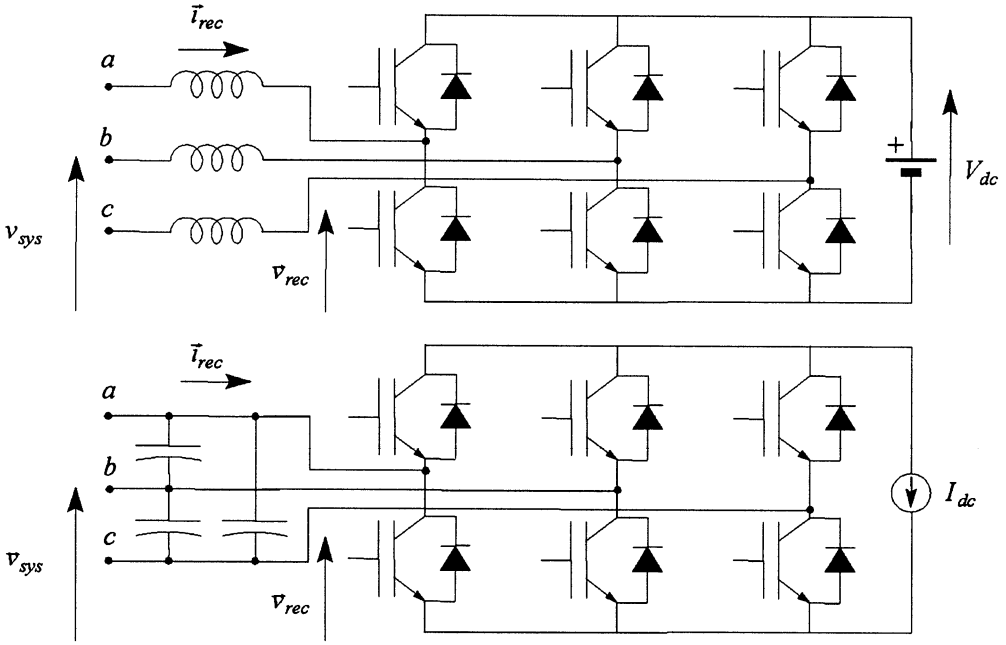

Fig. 7. Active rectifier with a voltage or current source on the dc side.

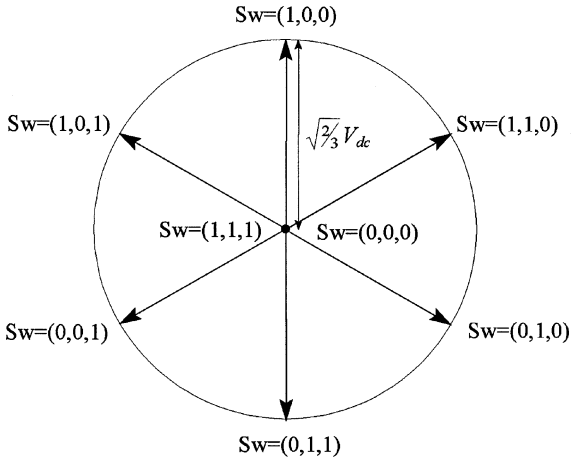

Fig. 8. Voltage spatial vector $\vec{v}_{\text{sec}}$ as function of the switching vector $\mathbf{Sw}$ for a rectifier bridge feeding a voltage source.

$$\mathbf{U} = \begin{bmatrix} 1 & 0 & 0 \\ 0 & 1 & 0 \\ 0 & 0 & 1 \end{bmatrix},\ \mathbf{S} = \begin{bmatrix} 1 & -\frac{1}{2} & -\frac{1}{2} \\ -\frac{1}{2} & 1 & -\frac{1}{2} \\ -\frac{1}{2} & -\frac{1}{2} & 1 \end{bmatrix}$$

$$\mathbf{C} = \begin{bmatrix} \cos\theta & \cos\left(\theta + \frac{2\pi}{3}\right) & \cos\left(\theta + \frac{4\pi}{3}\right) \\ \cos\left(\theta + \frac{4\pi}{3}\right) & \cos\theta & \cos\left(\theta + \frac{2\pi}{3}\right) \\ \cos\left(\theta + \frac{2\pi}{3}\right) & \cos\left(\theta + \frac{4\pi}{3}\right) & \cos\theta \end{bmatrix}.$$

Applying the space–vector transformation [11]–[13], the following model can be obtained in the stator frame:

$$\begin{bmatrix} \vec{\mathbf{v}}_s^s \\ \vec{\mathbf{v}}_r^s \end{bmatrix} = \begin{bmatrix} R_s & 0 \\ 0 & R_r \end{bmatrix} \begin{bmatrix} \vec{\mathbf{i}}_s^s \\ \vec{\mathbf{i}}_r^s \end{bmatrix} + \begin{bmatrix} L_s' & L_{sr}' \\ L_{sr}' & L_r' \end{bmatrix} p \begin{bmatrix} \vec{\mathbf{i}}_s^s \\ \vec{\mathbf{i}}_r^s \end{bmatrix} - j\dot{\theta} \begin{bmatrix} 0 & 0 \\ L_{sr}' & L_r' \end{bmatrix} \begin{bmatrix} \vec{\mathbf{i}}_s^s \\ \vec{\mathbf{i}}_r^s \end{bmatrix} \tag{18}$$

$$T_e = L_{sr}\Im m\left\{\vec{\mathbf{i}}_s^s \vec{\mathbf{i}}_r^{s*}\right\}. \tag{19}$$

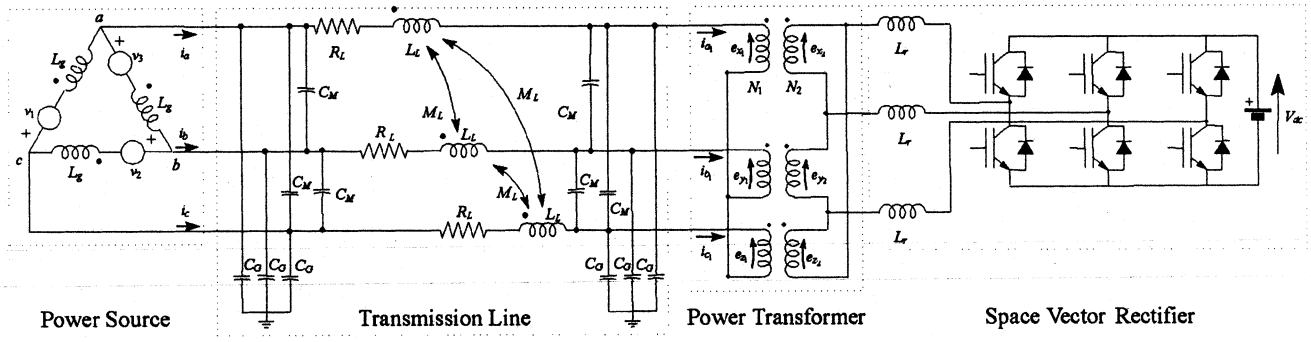

Fig. 9. Example power system.

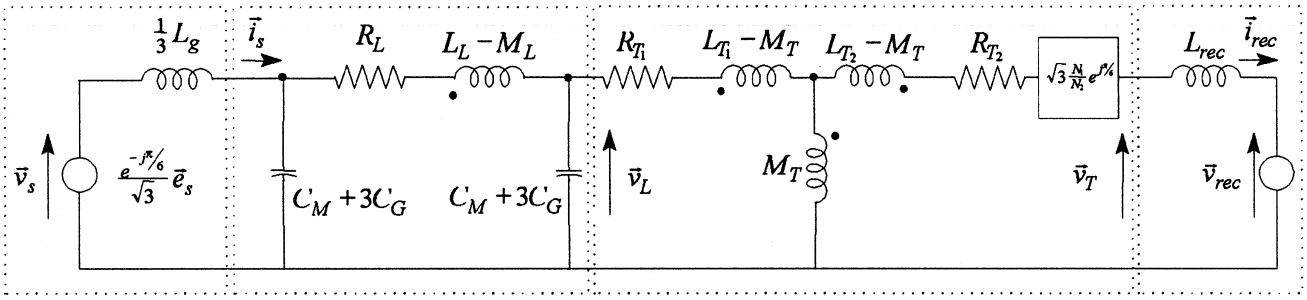

Fig. 10. Space–vector model of the example power system.

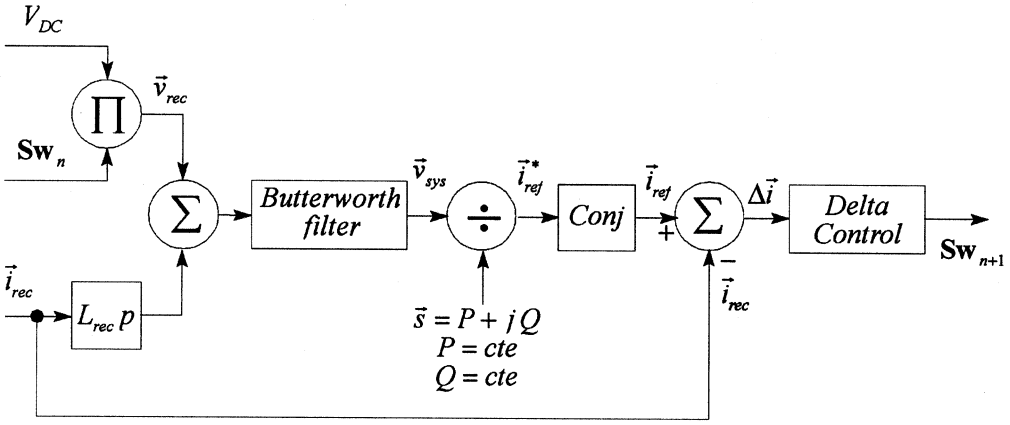

Fig. 11. Control scheme of the active rectifier.

TABLE I
NETWORK EXAMPLE PARAMETERS

L_g	R_L	$L_L - M_L$	$3C_M + C_G$	L_{rec}
0.03	0.005	0.05	0.1	0.2
R_{T_1}	R_{T_2}	L_{T_1}	L_{T_2}	M_T
0.005	0.005	100.05	100.05	100.00

Fig. 6 shows the equivalent circuit of the induction machine in stator reference frame. The model is valid for dynamic, steady-state, or harmonic analysis. Electromagnetic torque can be obtained by superposition of the instantaneous power in generating coefficients, divided by the shaft angular speed $\dot{\theta}$.

E. Synchronous Machine Model

Cylindrical or nonsalient rotor-synchronous machines can be modeled using (8) or (10). However, the model for the salient-pole-synchronous machine cannot be decoupled using space–vector transformation. This is due to the acyclic matrices in the salient-pole machine model. But the model can be simplified using any rotational transformation, such as Park's Transformation [2], [14], where the angular dependences of the inductance matrices are removed. However, a minimum of two independent axes are needed to model the machine [10], [12].

F. Rectifier Bridge Model

The space–vector model of a rectifier bridge can be derived assuming that three switches are on at any instant of time and

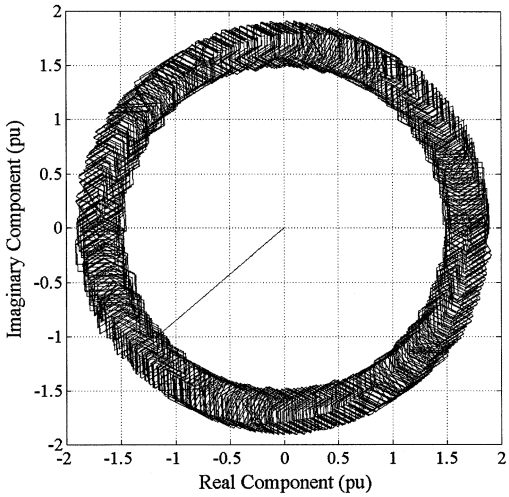

Fig. 12. Space vector of the power transformer's secondary side voltage.

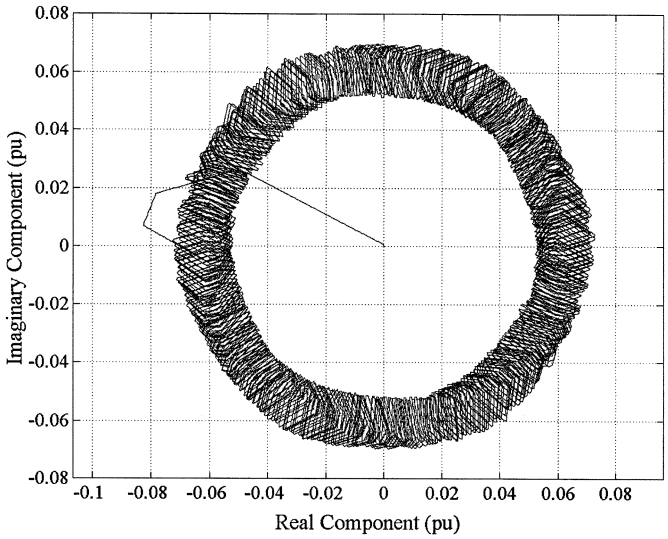

Fig. 13. Space vector of the power transformer's secondary side currents.

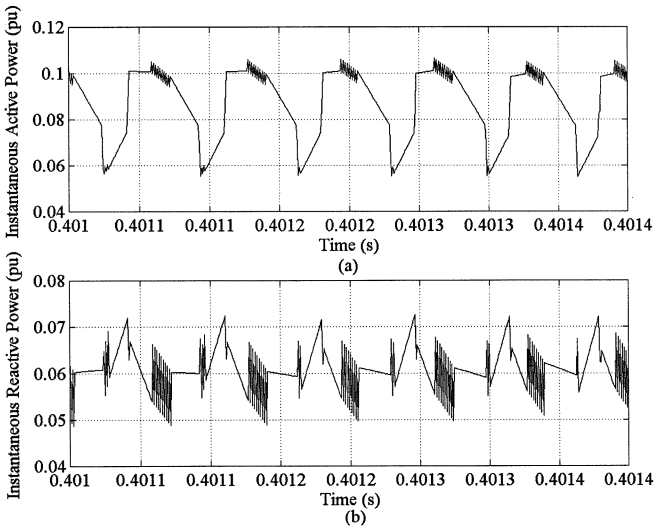

Fig. 14. (a) Instantaneous active power at the transformer's secondary. (b) Instantaneous reactive power at the transformer's secondary.

that the rectifier feeds a constant voltage or a constant current source (as shown in Fig. 7). When the rectifier feeds a voltage source, the states of the switches define the voltage space vector $\vec{v}_{\rm sec}$. With $\vec{v}_{\rm sec}$ and $\vec{v}_{\rm sys}$ known, the space vector of the ac current $\vec{i}_{\rm sec}$ can be obtained as

$$\vec{v}_{\rm sys} = \vec{v}_{\rm sec} + L_{\rm sec} p\vec{i}_{\rm sec}. \tag{20}$$

where $L_{\rm sec}$ is the inductance per-phase of the ac source. The voltage space vector $\vec{v}_{\rm sec}$ is given by

$$\begin{aligned}\vec{v}_{\rm sec} &= \sqrt{\frac{2}{3}}\left[1 \quad e^{j2\pi/3} \quad e^{j4\pi/3}\right] \cdot \begin{bmatrix} v_A \\ v_B \\ v_C \end{bmatrix} \\ &= \sqrt{\frac{2}{3}}\left[1 \quad e^{j2\pi/3} \quad e^{j4\pi/3}\right] \cdot \mathbf{Sw} \cdot V_{dc}. \end{aligned} \tag{21}$$

where $\mathbf{Sw}$ is a 3×1 vector representing the states of the switches and whose elements are "one" if the upper switch is on, and "zero" if the lower is on, for each phase. The rectifier voltage space vector $\vec{v}_{\rm sec}$ has only seven possible states (as shown in Fig. 8).

For a rectifier feeding a constant current source, the ac current space vector $\vec{i}_{\rm sec}$ has the same states as shown in Fig. 8 for the voltage space vector in a rectifier feeding a constant voltage source. Nevertheless, during the commutation intervals, the current space vector $\vec{i}_{\rm sec}$ cannot change instantaneously between two positions. There is a smoother variation along the space circle path caused by the capacitance $C_{\rm sec}$. During commutation, the line current changes continuously, reducing in magnitude in one phase and increasing in the other. Under these conditions, the magnitude of the current space vector $\left|\vec{i}_{\rm sec}\right|$ depends on the switching strategy. For example, in a delta-current-controlled bridge, the current space vector traces a circle at constant angular speed. In any other control scheme, a more detailed circuit analysis of the commutation process must be performed in order to determine the trajectory of the current space vector. The analysis of a power system with rectifier bridges requires an accurate modeling of the rectifier control scheme.

IV. Example Results

A. Active Rectifier Example

A simple power system with a delta-connected source, a medium-length transmission line, a wye–delta (Yd11) power transformer, and an active rectifier feeding as a voltage source are shown in Fig. 9. The space–vector model for this power system is shown in Fig. 10. The active and reactive power of the rectifier are controlled instantaneously using delta modulation of the current and is shown in Fig. 11. Model parameters (in per unit) used in this example are listed in Table I. The active power reference is 0.08, and the reactive power reference is 0.06 (lagging). Simulation in the time domain was performing using MATLAB by direct integration of the state equations.

The voltage and current space vectors at the transformer secondary are shown in Figs. 12 and 13, respectively. In the voltage space vector, the small circumvolution is caused by the voltage drop produced by the harmonics in the current.

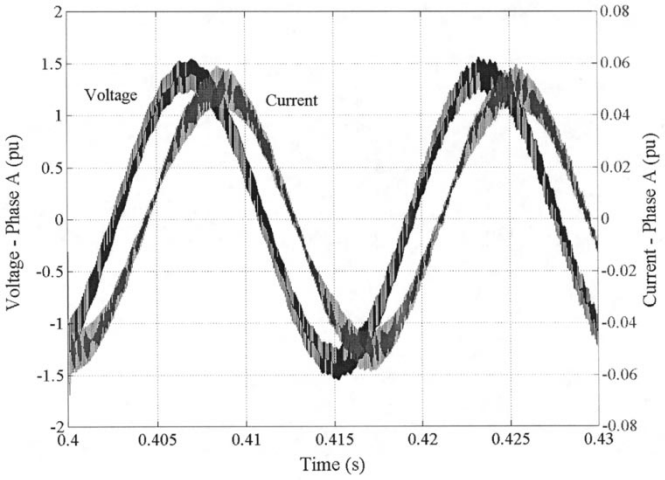

Fig. 15. Instantaneous voltage and current in one phase of the power transformer's secondary side. Power system simulation example, with transients and harmonics included.

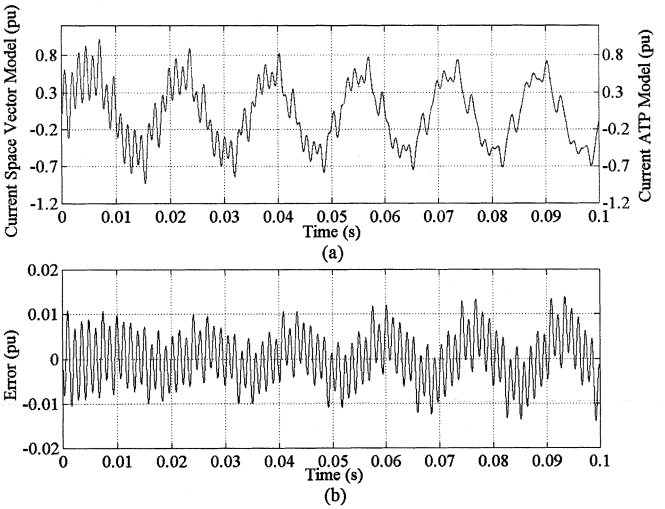

Fig. 16. (a) Instantaneous current in phase "a" of the load. ATP and space–vector models. (b) Instantaneous error between ATP and space–vector models.

The hexagonal space wave is generated by the switching of the rectifier bridge. The current space–vector is also affected by the harmonics, but the network response produces lower wave distortions. The instantaneous active and reactive power at the transformer secondary are shown in Fig. 14. The instantaneous active and reactive power have mean values that match the respective reference values, with oscillation due to harmonic currents and voltages. Instantaneous voltage and current in one phase of the transformer secondary are shown in Fig. 15.

B. Power System Simulation Example With Transients and Harmonics Included

A comparison between alternative-transients program (ATP) and space–vector models has been performed with a three-phase generation system [22]. A 115-kV short transmission line ($L_1 = L_2 = 10.6$ mH; $L_0 = 9.5$ mH) is connected to a 115-MVA wye–delta transformer (Yd1) 110/22 kV, $Z_{sc} = 8.52\%$. Transformer copper losses are 60.6 kW, and magnetizing current is 0.45% at rated voltage. The power transformer feeds a 7-MVA load with $p.f. = 0.8$ (lagging) at 22 kV and 1.89 MVAR of capacitive compensation. The voltage source is balanced and has fifth and seventh harmonics

$$v_a(t) = 1.3 \cdot \sin(\omega t) + 0.5 \cdot \sin(5\omega t) + 0.2 \cdot \sin(7\omega t).$$

The load current in phase "a" as generated by the three-phase ATP model and the proposed space–vector model using MATLAB are shown in Fig. 16(a). The error between the two models is shown in Fig. 16(b) and is less than 5% in the worst case. The space vector of the load current during steady state with harmonic distortion is shown in Fig. 17.

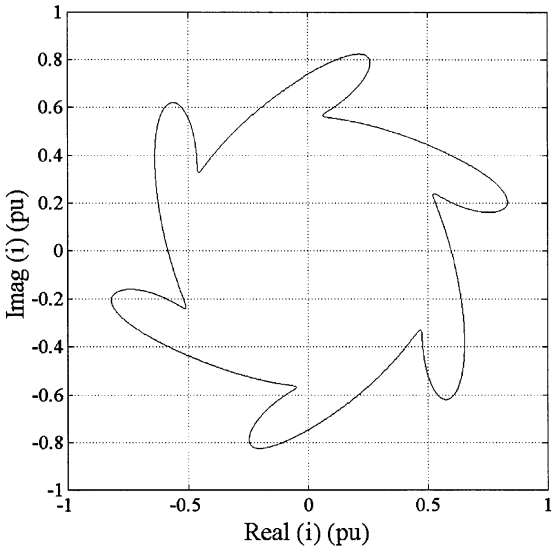

Fig. 17. Space vector of the load current in steady state.

V. Conclusion

In this paper, the space–vector transformation has been applied to analyze a power system. Space–vector models simplify the system representation and provide a better interpretation of polyphase circuits. Space–vector transformation is a useful tool to model a power system when power electronics converters are present. This technique can be applied under steady-state or transient conditions, and even when harmonics are present. Simulation examples including several circuit components (power source, transmission line, wye–delta power transformer, and active rectifier) have been provided to illustrate the advantage of the proposed method for power system analysis.

Space–vector variables can be used with several advantages in ATP routines or any other simulation programs to simplify polyphase circuits analysis with single-phase models valid under harmonics or transient conditions.

The main limitation of this method is that it is applicable only to symmetrical systems. Instantaneous symmetrical components method can be used to analyze unbalance systems.

Acknowledgment

The authors wish to express their gratitude to CONICIT (S1–97001762) and the Dean of Research and Development Bureau of the Simón Bolívar University (GID-04) for the

financial support provided for this work. The authors also wish to acknowledge their gratitude to V. Guzmán, M. I. Giménez, R. Tallam, and A. Ginart.

REFERENCES

[1] E. Clarke, *Circuit Analysis of AC Power Systems*. New York: Wiley, 1943, vol. I.
[2] R. H. Park, "Two-reaction theory of synchronous machines," *AIEE Trans.*, vol. 48, p. 716, 1929.
[3] C. L. Fortescue, "Method of the symmetrical coordinates applied to the solution of polyphase networks," *Trans. AIEE*, vol. 37, pp. 1027–1140.
[4] H. Karrenbauer, "Propagation of traveling waves on overhead lines for variation tower configuration and its effects on the shape of the recovery voltage for short line faults," Ph.D. dissertation, Munich, Germany, 1967.
[5] H. Edelmann, "Algebraic eigenvalue theory of components systems utilizing network symmetries," *Siemens Forschungs- und Entwicklungsberichte/Siemens Res. Devel. Rep.*, vol. 10, no. 6, pp. 351–356, 1981.
[6] H. W. Dommel and W. S. Meyer, "Computation of electromagnetic transients," *Proc. IEEE*, vol. 62, no. 7, pp. 983–993, 1974.
[7] J. Arrillaga, C. P. Arnold, and B. J. Harker, *Computer Modeling of Electrical Power System*. New York: Wiley, 1983.
[8] F. Blaschke, "The principle of field orientation as applied to the new transkvector close-loop control system for rotating-field machines," *Siemens Rev.*, vol. 34, pp. 217–220, 1972.
[9] W. Leonhard, *Control of Electrical Drives*. Belin, Germany: Springer-Verlag, 1985.
[10] S. Yamamura, *Spiral Vector Theory of AC Circuits and Machines*. New York: Oxford Univ. Press, 1992.
[11] A. Trzynadlowski, *The Field Orientation Principle in Control of Induction Motors*. Boston, MA: Kluwer Academic, 1994.
[12] D. Novotny and T. Lipo, *Vector Control and Dynamics of AC Drives*. New York: Oxford Univ. Press, 1996.
[13] J. M. Aller, "Simple matrix method to introduce space vector transformation and oriented field equations in electric machine courses," in *Proc. 1996 Int. Conf. Electrical Machines*, vol. 3, pp. 519–524.
[14] D. C. White and H. H. Woodson, *Electromechanical Energy Conversion*. New York: Wiley, 1959.
[15] Y. Nishida, O. Miyashita, T. Haneyoshi, H. Tomita, and A. Maeda, "A predictive instantaneous-current PWM controlled rectifier with AC-side harmonic current reduction," *IEEE Trans. Ind. Electron.*, vol. 44, pp. 337–343, June 1997.
[16] D. Shmilovitz, D. Czarkowski, Z. Zabar, and Y. Soo-Yeub, "A novel reversible boost rectifier with unity power factor," in *Proc. APEC '99*, vol. 1, 1999, pp. 363–368.
[17] T. Ohnuki, O. Miyashita, P. Lataire, and G. Maggetto, "Control of a three-phase PWM rectifier using estimate AC-side and DC-side voltage," *IEEE Trans. Power Electron.*, vol. 14, pp. 222–226, Mar. 1999.
[18] M. T. Madigan, R. W. Erickson, and E. H. Ismail, "Integrated high-quality rectifier-regulators," *IEEE Trans. Ind. Electron.*, vol. 46, pp. 749–758, Aug. 1999.
[19] H. Akagi and A. Nabae, "The p-q theory in three-phase systems under nonsinusoidal conditions," *Eur. Trans. Elec. Power Eng.*, vol. 3, no. 1, pp. 27–31, 1993.
[20] L. Cristaldi, A. Ferrero, J. Willems, M. Depenbrock, V. Staudt, and L. Czarnecki, "Mathematical foundations of the instantaneous power concepts: An algebraic approach," *Eur. Trans. Electrical. Power Eng.*, vol. 6, no. 5, pp. 305–314, 1996.
[21] J. M. Aller, A. Bueno, J. A. Restrepo, M. I. Giménez, and V. M. Guzmán, "Advantages of the instantaneous reactive power definitions in three-phase systems measurement," *IEEE Power Eng. Rev.*, vol. 19, no. 6, pp. 48–49, June 1999.
[22] H. W. Dommel, *Modeling Power Electronics in Power Systems Using EMTP. A Short Curse*. Vancouver, BC, Canada: Univ. British Columbia, 1993, pp. 22–23.

José M. Aller was born in Caracas, Venezuela in 1958. He received the Ing. degree in electrical engineering from Simón Bolívar University, Caracas, Venezuela, in 1980, the M.S. degree in electrical engineering from Universidad Central de Venezuela, Caracas, in 1982, and the Ph.D. degree in industrial engineering from Universidad Politécnica de Madrid, Madrid, Spain in 1993.

He has been a Lecturer at the Simón Bolívar University for 21 years, where he is currently a full-time Professor at the Energy Conversion Department. His research interests include space–vector application, electrical machine control, and power electronics.

Alexander Bueno was born in Caracas, Venezuela in 1971. He received the Ing. and M.S. degrees in electrical engineering from Universidad Simón Bolívar, Caracas, Venezuela, in 1993 and 1997, respectively.

He has been an Assistant Lecturer of electrical power engineering at the Industrial Technology Department, Simón Bolívar University for five years. Currently, his research interests include space–vector control applications, neural network estimators, and power electronics.

Tomás Pagá was born in Caracas, Venezuela in 1969. He received the Ing. and M.S. degrees in electrical engineering from Simón Bolívar University, Caracas, Venezuela, in 1994 and 1999, respectively.

He has been an Assistant Lecturer of electrical power engineering at the Energy Conversion Department, Simón Bolívar University for two years. Currently, his research interests include space–vector rectification, synchronous machine control, and power electronics.